Microwave tomography for breast cancer detection within a Variational Bayesian Approach

Leila Gharsalli, H Ayasso, Bernard Duchêne, Ali Mohammad-Djafari

MICROWAVE TOMOGRAPHY FOR BREAST CANCER DETECTION WITHIN A VARIATIONAL BAYESIAN APPROACH

L. Gharsalli, B. Duchêne, A. Mohammad-Djafari

Laboratoire des Signaux et Systèmes (L2S)
(UMR8506 : CNRS - SUPELEC - Univ Paris-Sud)
3 rue Joliot-Curie, 91190 Gif-sur-Yvette, France

H. Ayasso

GIPSA-LAB, Département Image Signal
(CNRS - Univ Joseph Fourier)
BP 46 - 38402, Saint Martin d'Hères, France

ABSTRACT

We consider a nonlinear inverse scattering problem where the goal is to detect breast cancer from measurements of the scattered field that results from its interaction with a known wave in the microwave frequency range. The modeling of the wave-object interaction is tackled through a domain integral representation of the electric field in a 2D-TM configuration. The inverse problem is solved in a Bayesian framework where the prior information is introduced via a Gauss-Markov-Potts model. A Variational Bayesian Approximation (VBA) technique is adapted to complex valued contrast and applied to compute the posterior estimators and reconstruct maps of both the permittivity and conductivity. Results obtained by means of this approach from synthetic data are compared with those given by a deterministic contrast source inversion method.

Index Terms— Inverse scattering problem, breast cancer detection, Gauss-Markov-Potts prior, Variational Bayesian Approximation.

1. INTRODUCTION

In last few years, a lot of work has been devoted to the application of microwave imaging to breast tumor detection [1, 2]. In fact, microwave imaging is an attractive alternative to X-ray mammography for detection of breast cancers because dielectric properties of tumors are notably different from that of healthy biological tissues and microwaves can be used to emphasize these differences.

Microwave tomography is a nonlinear inverse scattering problem where the goal is to retrieve a contrast function representative of the dielectric properties (permittivity and conductivity) of an unknown object, from measurements of the scattered field that results from its interaction with a known interrogating (incident) wave. When the object under test is small compared to the wavelength or is lowly contrasted with respect to the embedding, this inverse problem can be linearized in the framework of the first order weak scattering Born or Rytov approximations [3, 4]. However, as underlined above, it is not the case of the objects considered herein, as contrast can be high. In the early 90's, several deterministic inversion algorithms have been developed in order to deal with the nonlinear problem at hand in the case of microwave imaging, through an iterative minimization of a cost functional that expresses the discrepancy between the measured scattered fields and the fields computed by means of the current solution (the sought contrast) through a forward model based upon two coupled integral equations that link the observed scattered field to the contrast function [5, 6, 7].

Nonetheless, inverse scattering problems are known to be ill-posed, which means that a regularization is required prior to their resolution. Such a regularization is usually done by introducing *a priori* information on the object, which is not easy with the latter techniques as this information must be introduced in the functional to be minimized. The Bayesian framework allows us to take easily into account such an information. In fact, we know that the object under test is composed of a finite number of different materials distributed in compact regions, meaning that the sought image is composed of a finite number of homogeneous area. To account for this prior knowledge, a Gauss-Markov field with an hidden Potts label field, denoted hereafter as Gauss-Markov-Potts model, is proposed and a variational Bayesian approximation (VBA, [8]) is applied to obtain an estimator of the posterior law. This method has already been applied to optical diffraction tomography [9]. Its performances have been compared to Monte-Carlo Markov Chain (MCMC) methods that yield good results but are very costly in terms of computation time and technical difficulties [10, 11]. The originality of this work is to apply this approach to breast cancer detection where, contrarily to the case treated in [9], the unknown contrast is complex valued because biological media are lossy, which means that both permittivity and conductivity images have to be reconstructed. Hence the proposed Bayesian approach and the VBA method are adapted to the case of complex valued contrasts by assuming that permittivity and conductivity have the same segmentation, i.e. the same hidden field, but are independent conditionally to this hidden variable.

The rest of this paper is organized ad follows: section 2 presents the forward modeling of the problem. Then the

Bayesian framework is presented in section 3 and the variational approach is discussed in section 4. The method is applied to breast tumor detection in section 5 and compared to contrast source inversion method (CSI, [7]). Finally, some conclusions and perspectives are given in section 6.

2. FORWARD PROBLEM

We consider a 2-D configuration in a transverse magnetic polarization case where the object under test is supposed to be cylindrical, of infinite extension along the z axis and illuminated by a line source whose location can be varied and that operates at several discrete frequencies in the range 0.5 GHz - 3 GHz. This source generates an incident electric field E^{inc} polarized along the z axis with an $\exp(-i\omega t)$ implicit time dependence. The object is supposed to be contained in a test domain $\mathcal{D}$ and the different media are characterized by their propagation constant $k(\boldsymbol{r})$ such that $k(\boldsymbol{r})^2 = \omega^2\epsilon_0\epsilon_r(\boldsymbol{r})\mu_0 + i\omega\mu_0\sigma(\boldsymbol{r})$, where ω is the angular frequency, ϵ_0 and μ_0 are the permittivity and the permeability of free space, respectively, $\boldsymbol{r} \in \mathcal{D}$ is an observation point and $\epsilon_r(\boldsymbol{r})$ and $\sigma(\boldsymbol{r})$ are the relative permittivity and conductivity of the medium. We now consider a contrast function χ defined in $\mathcal{D}$ and null outside the object, such that $\chi(\boldsymbol{r}) = (k(\boldsymbol{r})^2 - k_1^2)/k_1^2$, where k_1 is the propagation constant of the embedding medium and we define $w(\boldsymbol{r})$ as the Huygens type sources induced within the target by the incident wave, i.e. $w(\boldsymbol{r}) = \chi(\boldsymbol{r})E(\boldsymbol{r})$ where $E(\boldsymbol{r})$ is the total field in the target. By applying Green's theorem to the Helmholtz wave equations satisfied by the fields and by accounting for boundary and radiation conditions, we obtain two coupled contrast source integral equations, whose first one, denoted as *observation* equation, is a first-kind Fredholm integral equation that relates the scattered field $y(\boldsymbol{r})$ observed on a measurement domain $\mathcal{S}$ ($\boldsymbol{r} \in \mathcal{S}$), which results from the interaction between the object and the interrogating wave E^{inc}, to the induced sources $w(\boldsymbol{r})$:

$$y(\boldsymbol{r}) = k_1^2 \int_{\mathcal{D}} G(\boldsymbol{r}, \boldsymbol{r}')\, w(\boldsymbol{r}')\, \mathrm{d}\boldsymbol{r}', \tag{1}$$

where $G(\boldsymbol{r}, \boldsymbol{r}')$ is the 2-D Green's function. The second equation, the so-called *coupling* equation, relates the unknown total field E in the object to the induced sources $w(\boldsymbol{r})$:

$$E(\boldsymbol{r}) = E^{inc}(\boldsymbol{r}) + k_1^2 \int_{\mathcal{D}} G(\boldsymbol{r}, \boldsymbol{r}')\, w(\boldsymbol{r}')\, \mathrm{d}\boldsymbol{r}'. \tag{2}$$

The forward problem then consists in first solving (2) for E, knowing χ, then solving (1) for y knowing w. This is done from discrete counterparts of the above equations obtained by means of a method of moments [12] with pulse-basis and point matching. The test domain $\mathcal{D}$ is then partitioned into $N_{\mathcal{D}}$ elementary square pixels small enough in order to consider the field and the contrast as constant over each of them.

3. BAYESIAN FRAMEWORK AND PRIOR INFORMATION

Let us denote as $\boldsymbol{E}$, $\boldsymbol{\chi}$ and $\boldsymbol{w}$ the vectors that contain the values of $E(\boldsymbol{r}')$, $\chi(\boldsymbol{r}')$ and $w(\boldsymbol{r}')$ at the centers $\boldsymbol{r}'$ of the pixels ($\boldsymbol{r}' \in \mathcal{D}$), as $\boldsymbol{y}$ the vector containing the values of the scattered field $y(\boldsymbol{r})$ at the measurement points $\boldsymbol{r}$ ($\boldsymbol{r} \in \mathcal{S}$) and as $\boldsymbol{G}^o$ and $\boldsymbol{G}^c$ huge matrices whose elements result from the integration of the Green's function over the elementary pixels (their expressions are given in [9]). Let us also introduce a subscript n that accounts for the different frequencies (f) and source positions (ν) and two variables, $\boldsymbol{\epsilon}$ and $\boldsymbol{\xi}$, that account for the model and measurement errors and that are supposed to be centered and white and to satisfy Gaussian laws (i.e., $\boldsymbol{\epsilon}_n \sim \mathcal{N}(\boldsymbol{0}, v_\epsilon \mathbf{I})$ and $\boldsymbol{\xi}_n \sim \mathcal{N}(\boldsymbol{0}, v_\xi \mathbf{I})$). By rewriting (2) in terms of the contrast sources, we get the following discrete counterparts of the observation and coupling equations:

$$\boldsymbol{y}_n = \boldsymbol{G}_f^o\, \boldsymbol{w}_n + \boldsymbol{\epsilon}_n \tag{3}$$

$$\boldsymbol{w}_n = \boldsymbol{X}_f\, \boldsymbol{E}_n^{inc} + \boldsymbol{X}_f\, \boldsymbol{G}_f^c\, \boldsymbol{w}_n + \boldsymbol{\xi}_n, \tag{4}$$

where $\boldsymbol{X}_f = \mathrm{diag}(\boldsymbol{\chi}_f)$. The inverse problem consists, then, in estimating the contrast $\boldsymbol{\chi}$, or more precisely the relative permittivity ϵ_r and the conductivity σ, from the scattered fields $\boldsymbol{y}$, given the incident fields $\boldsymbol{E}^{inc}$. It can be noted that, the induced sources $\boldsymbol{w}$ being unknown, they have to be estimated at the same time as $\boldsymbol{\chi}$.

It is well known that inverse scattering problems are ill-posed. This means that they must be regularized, which is usually done by introducing *a priori* information on the sought solution. The Bayesian framework is particularly well suited for that, as it allows us to introduce such an information in a really easy way. In the present case, the information that we would like to account for is that the object is composed of a finite number K of different materials distributed in compact homogeneous regions. This prior information is introduced by means of a hidden variable $z(\boldsymbol{r})$, associated to each pixel $\boldsymbol{r}$, that represents a segmentation of the unknown object. This label defines different classes of materials and pixels with a given class k can be characterized by a contrast that satisfies a Gaussian distribution:

$$p(\chi(\boldsymbol{r})|z(\boldsymbol{r}) = k) = \mathcal{N}(m_k, v_k), \qquad k = 1, \ldots, K, \tag{5}$$

with mean value m_k and variance v_k. The information that the different materials are distributed in compact homogeneous regions is accounted for by means of a Potts-Markov model on $\boldsymbol{z}$ that expresses the spatial dependence between the neighboring pixels:

$$p(\boldsymbol{z}|\lambda) = \frac{1}{T(\lambda)} \exp\left\{ \lambda \sum_{\boldsymbol{r} \in \mathcal{D}} \sum_{\boldsymbol{r}' \in V_{\boldsymbol{r}}} \delta\left(z(\boldsymbol{r}) - z(\boldsymbol{r}')\right) \right\}, \tag{6}$$

where $z = \{z(\boldsymbol{r}), \boldsymbol{r} \in \mathcal{D}\}$ represents the image of the labels (segmentation), λ is a parameter that determines the correlation between neighbors (herein $\lambda = 1$), $T(\lambda)$ is a normalization factor and $V_{\boldsymbol{r}}$ is a neighborhood of $\boldsymbol{r}$, herein made of the four nearest pixels.

It can be noted that a semi-supervised context is considered herein as K is supposed to be known, whereas the contrast $\boldsymbol{\chi}$, the induced currents $\boldsymbol{w}$, the segmentation $\boldsymbol{z}$ and the hyper-parameters of the model $\psi = \{\boldsymbol{m}, \boldsymbol{v}, v_\epsilon, v_\xi\}$ are estimated simultaneously. We apply the Bayes formula to get the joint posterior distribution of the unknowns:

$$\begin{aligned} p(\boldsymbol{\chi}, \boldsymbol{w}, \boldsymbol{z}, \boldsymbol{\psi}|\boldsymbol{y}) \quad &\propto \quad p(\boldsymbol{y}|\boldsymbol{w}, v_\epsilon)\, p(\boldsymbol{w}|\boldsymbol{\chi}, v_\xi)\, p(\boldsymbol{\chi}|\boldsymbol{z}, \boldsymbol{m}, \boldsymbol{v}) \\ &\times \quad p(\boldsymbol{z}|\lambda)\, p(\boldsymbol{m}|\mu_0, \tau_0)\, p(\boldsymbol{v}|\eta_0, \phi_0) \\ &\times \quad p(v_\epsilon|\eta_\epsilon, \phi_\epsilon)\, p(v_\xi|\eta_\xi, \phi_\xi). \end{aligned} \tag{7}$$

The expressions of $p(\boldsymbol{y}|\boldsymbol{w}, v_\epsilon)$ and $p(\boldsymbol{w}|\boldsymbol{\chi}, v_\xi)$, that appear in the above equation, are derived from equations (3) and (4), the expression of $p(\boldsymbol{\chi}|\boldsymbol{z}, \boldsymbol{m}, \boldsymbol{v})$ is derived from equations (5), whereas $p(\boldsymbol{z}|\lambda)$ is given in (6) and we assign the following conjugate prior laws to the hyper-parameters:

$$\begin{aligned} p(m_k) = \mathcal{N}(\mu_0, \tau_0), \quad p(v_k) = \mathcal{IG}(\eta_0, \phi_0) \\ p(v_\epsilon) = \mathcal{IG}(\eta_\epsilon, \phi_\epsilon), \quad p(v_\xi) = \mathcal{IG}(\eta_\xi, \phi_\xi), \end{aligned} \tag{8}$$

where $\mathcal{N}(m, v)$ and $\mathcal{IG}(\alpha, \beta)$ stand for Gaussian and inverse-gamma distributions, respectively, and μ_0, τ_0, η_0, ϕ_0, η_ϵ, ϕ_ϵ, η_ξ and ϕ_ξ are meta-hyper-parameters appropriately set to obtain almost non-informative prior distributions.

From equation (7), different inferences can be done on the unknowns. The usual way is to define a point estimator such as the joint maximum *a posteriori* (JMAP) or the posterior mean (PM). Generally, easy expressions for any of these two estimators are very hard to obtain. Hence, we approximate the posterior law in an analytic way by means of the variational Bayesian approach.

4. VARIATIONAL BAYESIAN APPROXIMATION

The outline of the variational Bayesian method (VBA, [8]) is to approximate the joint posterior distribution $p(\boldsymbol{x}|\boldsymbol{y})$, where $\boldsymbol{x} = \{\boldsymbol{\chi}, \boldsymbol{w}, \boldsymbol{z}, \boldsymbol{\psi}\}$, by a separable law $q(\boldsymbol{x}) = \prod_i q(\boldsymbol{x}_i)$ which is as close to the posterior distribution as possible in terms of the Kullback-Leibler divergence. It can be noted that minimizing the KL divergence is equivalent to maximizing the free negative energy derived from statistical physics:

$$\mathcal{F}(\boldsymbol{q}) = \int_{\mathcal{R}^N} q(\boldsymbol{x}) \ln \left(\frac{p(\boldsymbol{y}, \boldsymbol{x})}{q(\boldsymbol{x})} \right) \mathrm{d}\boldsymbol{x}. \tag{9}$$

We can thus summarize the objective of VBA by:

$$\text{find } \boldsymbol{q}^{opt} = \arg\max_{\boldsymbol{q}} \mathcal{F}(\boldsymbol{q}). \tag{10}$$

Then, assuming the separability ($q(\boldsymbol{x}) = \prod_i q(\boldsymbol{x}_i)$), we can obtain an analytic form for $\boldsymbol{q}$:

$$q(\boldsymbol{x}_i) \propto \exp\left\{ \langle \ln(p(\boldsymbol{x}, \boldsymbol{y})) \rangle_{\prod_{j \neq i} q(\boldsymbol{x}_j)} \right\}. \tag{11}$$

Now, by considering the joint posterior distribution (7), we choose a strong separation form:

$$q(\boldsymbol{x}) = q(v_\epsilon) q(v_\xi) \prod_i q(\chi_i) q(w_i) q(z_i) \prod_k q(m_k) q(v_k).$$

Then we apply the optimal form (equation (11)), which leads to the following parametric distributions:

$$\begin{aligned} q(\boldsymbol{w}) = \mathcal{N}(\widetilde{\boldsymbol{m}}_w, \widetilde{\boldsymbol{V}}_w), \qquad & q(\boldsymbol{\chi}) = \mathcal{N}(\widetilde{\boldsymbol{m}}_\chi, \widetilde{\boldsymbol{V}}_\chi), \\ q(m_k) = \mathcal{N}(\widetilde{\mu}_k, \widetilde{\tau}_k), \qquad & q(v_k) = \mathcal{IG}(\widetilde{\eta}_k, \widetilde{\phi}_k), \\ q(v_\epsilon) = \mathcal{IG}(\widetilde{\eta}_\epsilon, \widetilde{\phi}_\epsilon), \qquad & q(v_\xi) = \mathcal{IG}(\widetilde{\eta}_\xi, \widetilde{\phi}_\xi), \end{aligned}$$

$$q(\boldsymbol{z}) = \widetilde{\boldsymbol{\zeta}}_k \propto exp\left(\lambda \sum_{\boldsymbol{r} \in \mathcal{D}} \sum_{\boldsymbol{r}' \in \mathcal{V}(\boldsymbol{r})} \widetilde{\zeta}(\boldsymbol{r}') \right), \tag{12}$$

where the expressions of the tilted shaping parameters are detailed in [9]. It can be noted that these parameters are mutually dependent and can only be computed in an iterative way.

The initial values of the unknowns $\boldsymbol{\chi}^{(0)}$ and $\boldsymbol{w}^{(0)}$ are obtained by backpropagating the scattered field data from the measurement domain $\mathcal{S}$ onto the test domain $\mathcal{D}$, whereas the initial values of the segmentation $\boldsymbol{z}^{(0)}$ are given by *K-means* clustering [13], with empirical estimators for the hyperparameters $\boldsymbol{\psi}^{(0)}$. Here, given the fact that the contrast is complex valued, first the real part is segmented and, then, the same segmentation is used to initialize the imaginary part.

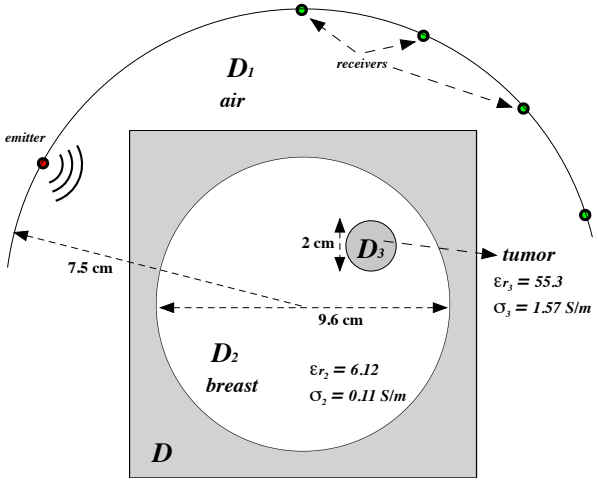

Fig. 1. The measurement configuration

5. APPLICATION AND RESULTS

The above method is applied to microwave imaging of a simulated breast supposed to be affected by a tumor (see Fig.1). The breast (domain $\mathcal{D}_2$) is of circular cross-section with a diameter of 9.6 cm. It is placed in air (domain $\mathcal{D}_1$) and its relative dielectric permittivity and conductivity are respectively equal to $\epsilon_r = 6.12$ and $\sigma = 0.11$ Sm^{-1}. The tumor (domain $\mathcal{D}_3$) is also of circular cross-section with a diameter of 2 cm and its relative dielectric permittivity and conductivity are respectively equal to $\epsilon_r = 55.3$ and $\sigma = 1.57$ Sm^{-1}. The source illuminates the breast from 16 various angular positions uniformly distributed around a circle of radius 7.5 cm centered at the origin and at 6 different frequencies in the band 0.5 - 3 GHz. For each frequency and illumination angle, 32 measurements of the scattered field are performed at angular positions also uniformly distributed around the same circle. It can be noted that, in order to avoid committing a so-called

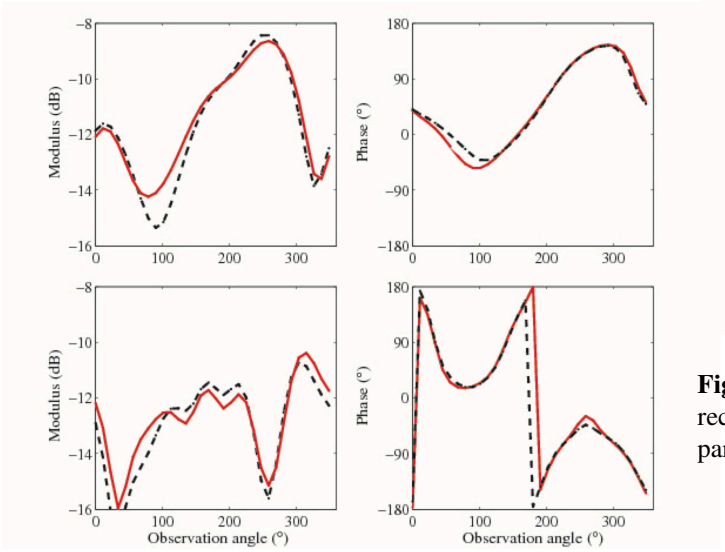

Fig. 2. Amplitude (left) and phase (right) of the scattered fields computed by means of the data model (red full line) and by means of the model used for inversion (black dashed line) at two frequencies: 1.5 GHz (up) and 2.5 GHz (down).

"inverse crime" in the sense of [14], which would consist in testing the inversion algorithm on data obtained by means of a model closely related to that used in the inversion, the synthetic data of the inverse problem are computed by means of a forward model (the data model) rather different from the one described in section 2. Indeed, whereas in the latter the object under test is the breast affected by the tumor, in the former it consists only in the tumor, the breast and the air being then considered as a cylindrically stratified embedding medium and the Green's function modified consequently. For inversion, the test domain $\mathcal{D}$ is a 12.16 cm sided square partitioned into 64×64 square pixels with side $\delta = 1.9$ mm. Figure 2 displays the scattered fields obtained by means of the two models when the breast is illuminated by a source located at 90° and operating at two frequencies: 1.5 GHz and 2.5 GHz. It can be observed that the results fit relatively well.

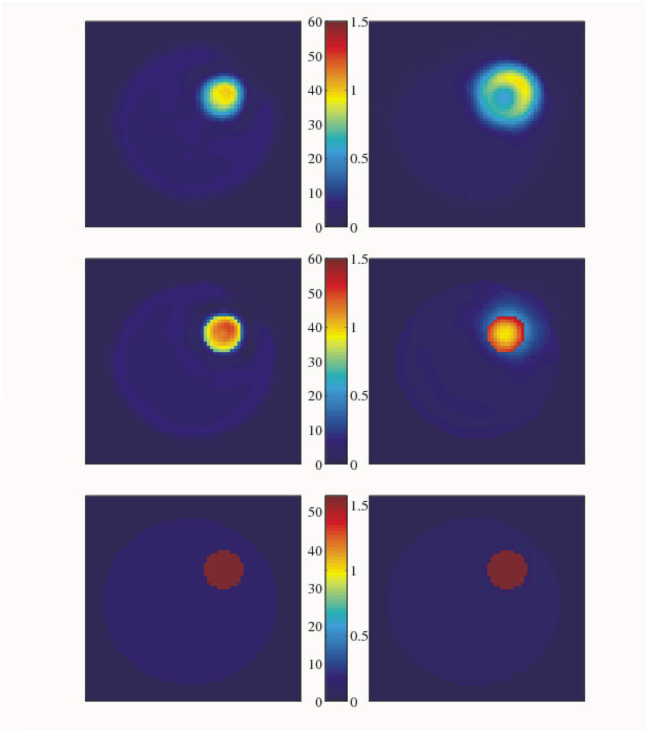

Fig. 3. Maps of the permittivity (left) and conductivity (right) reconstructed by means of CSI (up) and VBA (middle) compared to the real object (down).

Figure 3 displays maps of the permittivity and conductivity reconstructed by means of CSI after 500 iterations and by means of VBA after 4000 iterations, the latter being previously initialized by a few CSI iterations. The quality of reconstruction is significantly improved with VBA, especially for the conductivity, as compared to CSI which gives good results but with an insufficient resolution. Figure 4 displays the profiles reconstructed with both methods along an horizontal line crossing the center of the tumor and evidences the fact that VBA outperforms CSI, particularly with respect to the conductivity profile.

6. CONCLUSION

In this paper, microwave imaging for breast cancer detection is tackled in a Bayesian framework with a Gauss-Markov-Potts prior. A Variational Bayesian Approach (VBA) is used to approximate posterior with a free-form distribution with

respect to complex quantities as both permittivity and conductivity maps have to be retrieved. The results obtained by means of this approach show its effectiveness. Good results have been obtained concerning the retrieved permittivity, conductivity and geometry of the object and it has been shown that VBA performs better than the CSI deterministic inversion method. The drawback of VBA is that, as CSI, it can be considered as a local optimization algorithm that can be trapped in suboptimal solutions corresponding to local minima, contrarily to MCMC Bayesian approaches based upon stochastic sampling. However VBA is much faster than the latter (50 times faster for the configurations studied in [9]), and its speed of convergence can still be improved by applying a gradient like variational Bayesian method [15]. Finally, the application of the above method to laboratory controlled data is under investigation.

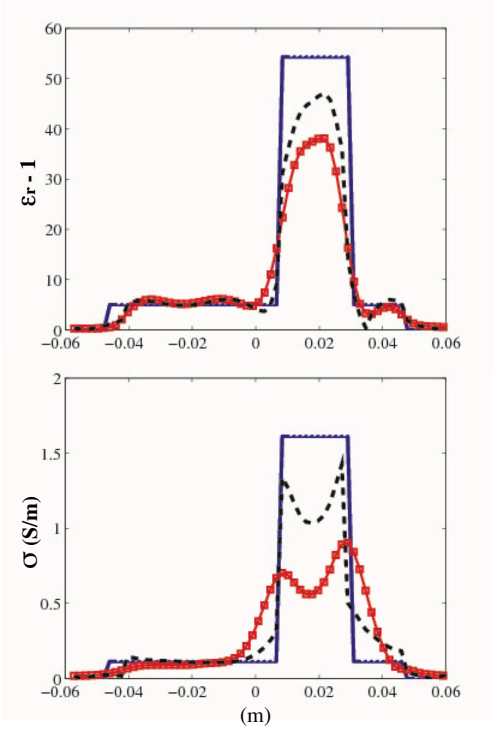

Fig. 4. Permittivity (up) and conductivity (down) profiles reconstructed by means of CSI (red squares) and VBA (black dashed line) compared to real profiles (blue full line).

7. REFERENCES

[1] T. Henriksson, *Contribution to quantitative microwave imaging techniques for biomedical applications*, Ph.D. thesis, Université Paris-Sud 11 - Mälardalen University, 2009.

[2] P. A. Barrière, *Développement d'algorithmes d'inversion rapides et propositions relatives à la configuration du montage de mesures dans un contexte de tomographie micro-onde appliquée à la détection du cancer du sein*, Ph.D. thesis, Ecole centrale de Nantes, 2008.

[3] A. J. Devaney, "A computer simulation study of diffraction tomography," *IEEE Trans. Biomed. Eng.*, vol. BME-30, no. 7, pp. 377–386, 1983.

[4] F. J. Paoloni, "Implementation of microwave diffraction tomography for measurement of dielectric constant distribution," *Microwaves, Antennas Propag., IEE Proceedings H*, vol. 134, no. 7, pp. 25–29, 1987.

[5] N. Joachimowicz, C. Pichot, and J. P. Hugonin, "Inverse scattering: an iterative numerical method for electromagnetic imaging," *IEEE Trans. Antennas Propag.*, vol. AP-39, no. 12, pp. 1742–1752, 1991.

[6] R. E. Kleinman and P. M. van den Berg, "A modified gradient method for two-dimensional problems in tomography," *J. Comput. Appl. Math.*, vol. 42, pp. 17–35, 1992.

[7] P. M. van den Berg and R. E. Kleinman, "A contrast source inversion method," *Inverse Problems*, vol. 13, no. 6, pp. 1607–1620, 1997.

[8] V. Smídl and A. Quinn, *The Variational Bayes Method in Signal Processing*, Springer Verlag, Berlin, 2006.

[9] H. Ayasso, B. Duchêne, and A. Mohammad-Djafari, "Optical diffraction tomography within a variational Bayesian framework," *Inverse Problems in Science and Engineering*, vol. 20, no. 1, pp. 59–73, 2012.

[10] O. Féron, B. Duchêne, and A. Mohammad-Djafari, "Microwave imaging of inhomogeneous objects made of a finite number of dielectric and conductive materials from experimental data," *Inverse Problems*, vol. 21, no. 6, pp. S95–S115, 2005.

[11] H. Ayasso, B. Duchêne, and A. Mohammad-Djafari, "Bayesian inversion for optical diffraction tomography," *J. Modern Opt.*, vol. 57, no. 9, pp. 765–776, 2010.

[12] W. C. Gibson, *The Method of Moments in Electromagnetics*, Chapman & Hall/CRC, 2008.

[13] J. B. MacQueen, "Some methods for classification and analysis of multivariate observations," in *Proc. 5th Berkeley Symp. Math. Statistics and Probability*. 1967, vol. 1, pp. 281–297, Univ. California Press.

[14] D. Colton and R. Kress, *Inverse Acoustic and Electromagnetic Scattering Theory*, Springer, New York, 1992.

[15] A. Fraysse and T. Rodet, "A gradient-like variational Bayesian algorithm," *Statistical Signal Processing Workshop (SSP)*, pp. 605–608, june 2011.